IOP Conf. Series: Materials Science and Engineering **274** (2017) 012121 doi:10.1088/1757-899X/274/1/012121

Dynamic wear evolution of steel wires during multi-axial fretting-fatigue

Dagang Wang*, Jun Zhang, Xiaowu Li, Dekun Zhang

School of Mechatronic Engineering, China University of Mining and Technology, Xuzhou 221116, China

*Corresponding author e-mail: wangdg@cumt.edu.cn

Abstract. In order to study the dynamic wear evolution of steel wires during multi-axial fretting-fatigue, experiments were carried out on a self-made multi-axial fretting fatigue test rig. The results show that the maximum length, maximum width, area and depth of wear scar will increase with the fatigue cycles, and the cross angle decreases from 11° to 4° with increasing fatigue cycles. The wear coefficient increases quickly at first and then tends to be stabilized when fatigue cycles increases from 5000 to 20000.

1. Introduction

Ropes have been widely employed in various engineering applications due to their capacity to support large axial loads with comparatively small bending or torsional stiffness [1,2]. During hoisting, ropes are subjected to cyclic stretching, bending and torsional loads[3,4], which will result in the cyclic tension-torsional stress of steel wires in ropes along with the relative displacements between them, and thus the dynamic tension-torsion stress and relative displacements will induce a combination of tensile and torsional fretting-fatigue(multi-axial fretting-fatigue) [5]. The wear of the steel wires during multi-axial fretting-fatigue will reduce the area of rope cross-section and thereby accelerate the failure of hoisting rope [6], which will cause severe safety accidents of hoist crash and casualties as the hoisting rope is a key component of transmission in a hoisting system [7]. Therefore, the study of dynamic wear evolution of steel wires during multi-axial fretting-fatigue is of great significance to the safety and reliability of the hoisting system in deep coal mine.

2. Experiment

In order to evaluate multi-axial fretting fatigue behaviors of steel wire in hoisting rope, a self-made multi-axial fretting fatigue test rig of steel wire was employed. The test rig can dynamically record the fatigue load, torque, torsion angle, contact load and tangential force between contacting wires, and the relative displacement. The test rig can be found in Fig 1.

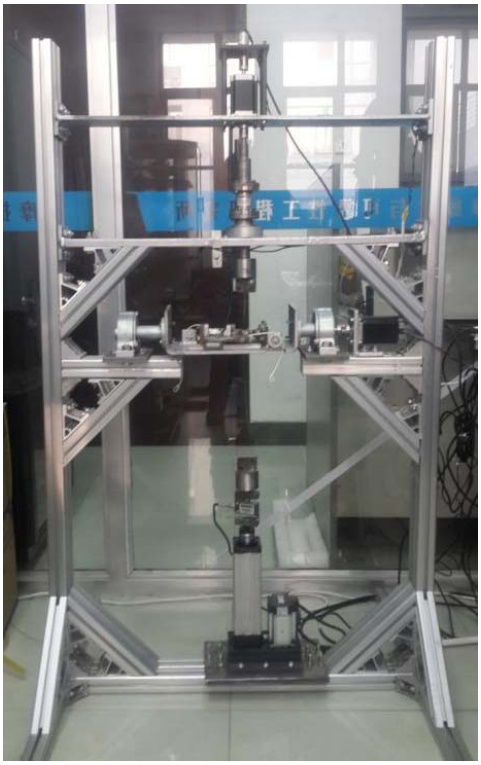

Fig 1. Schematic diagram of the mul-tiaxial fretting fatigue test rig of steel wire

Table I. Chemical composition of steel wire

Elements	Zn	C	Mn	Si	Ni	Fe
wt, %	4.53	0.84	0.39	0.02	0.01	其余

Table II. Multi-axial fretting fatigue test parameters

Fretting amplitude, D (μm)	Stress ratio	Mean stress (MPa)	Crossing angle(°)	Torsion angle (°)	Contact load, F_n(N)	Frequency, f (Hz)	Fatigue cycles, N
±100	0.5	190.5	90	±4	25	5	5000, 10000, 15000, 20000

Steel wires in hoisting rope are chosen as the research object. Those wires are manufactured by the cold drawing process of high quality carbon structural steel. They are cylindrical with the diameter of 1 mm and length of 400 mm. The chemical composition (in wt %) of the wire material is shown in Table I. The mul-tiaxial fretting fatigue test parameters are shown in Table II. Morphologies of wear scars of fatigue wires during multi-axial fretting-fatigue at distinct fatigue cycles were observed to explore multi-axial fretting fatigue wear mechanism employing the scanning electron microscope.

3. Dynamic Evolution of Wear

3.1. Evolution of Wear Scar Profile

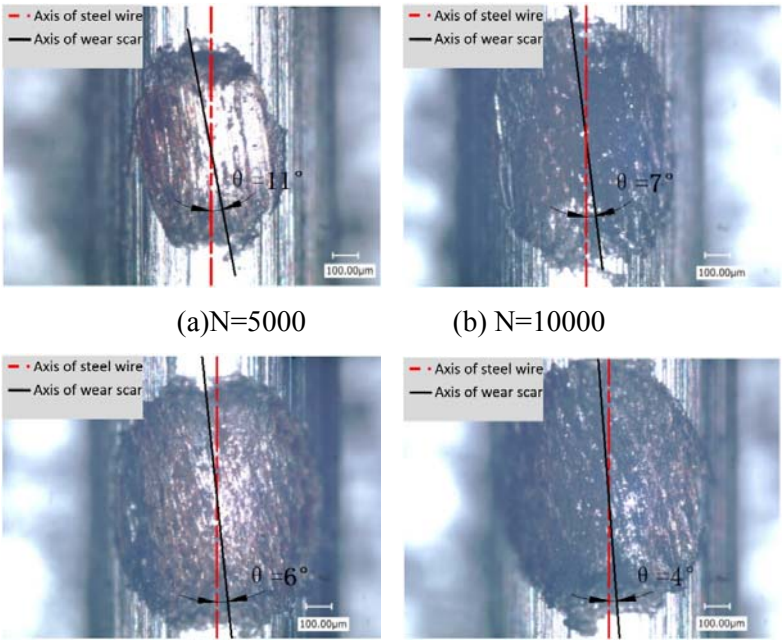

(a)N=5000 (b) N=10000

(c)N=15000 (d) N=20000

Fig 2. Wear scar morphologies of fatigue wires at different fatigue cycles

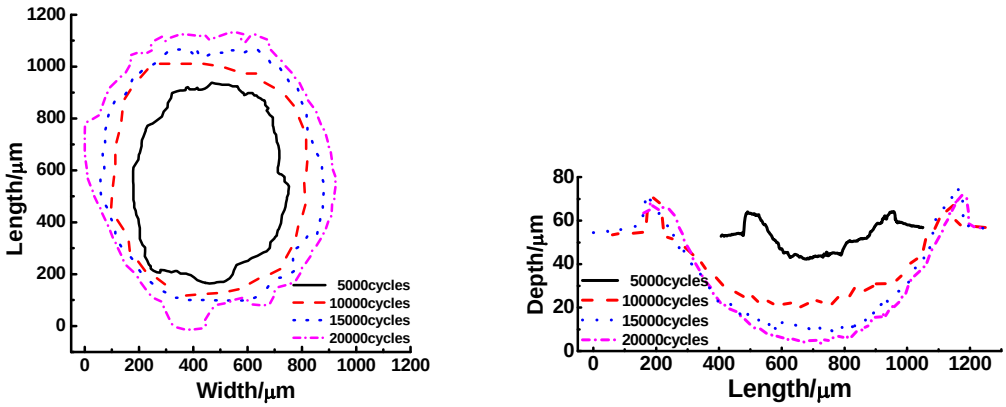

(a)Front wear scar profile (b) Side wear scar profile

Fig 3. Evolution of wear scar profile of fatigue wires at different fatigue cycles

Table III. Maximum lengths and widths, and areas of wear scars at different fatigue cycles

Fatigue cycles	5000	10000	15000	20000
Maximum length (L,μm)	768	850	969	1042
Maximum width (a,μm)	585	706	812	933
Maximum depth (h,μm)	18	36	46	53
Area ($\pi \cdot L \cdot a$)/4,μm^2)	352863	471317	617973	763553
Area difference (μm^2)		118454	146656	145580

Fig 2 shows the wear scar morphologies of fatigue wires at different fatigue cycles. As shown in Fig 2, the profile of wear scar present an irregular elliptical profile, and the major axis shows a cross angle θ with the axis of the fatigue steel wire. The cross angle decreases from 11° to 4° with the increasing of fatigue cycles, reason for this is that the main contact status is slip rather than adhesion, the torsional component induces a larger torsion angle between steel wires[8], i.e. a larger cross angle θ. As the fatigue

cycles increase, the relative slips between contact wires decreases and the adhesive zone increases, so the effect of torsional component reduces[8], which results in the decline of cross angle θ. Fig 3 and Table III show that with the increasing of fatigue cycles, the maximum length, maximum width, area and depth of wear scar increase, these are consistent with the evolution of friction coefficient in Fig 6.

3.2. Wear Coefficients

To establish the geometric model of wear scar, polynomial fitting of wear depth profiles of fatigue wires in tests at different fatigue cycles were shown in Fig 4. As the fatigue cycles increase from 5000 to 20000, the Adj.R-Square of polynomial fitting increases from 0.930 to 0.986, so the side profiles of wear scar can be thought as parabolic shape.

Fig 4 Polynomial fitting of wear depth profiles of fatigue wires in tests at different fatigue cycles

Based on the parabolic shaped side profiles of wear scar and the cross angle θ between the major axis of wear scar and the axis of steel wire, the geometric model of the fatigue steel wire wear scar was established as shown in Fig 5. In Fig 5, L is the maximum length of wear scar, h is the maximum depth of wear scar, origin of coordinate was set at the crossing point of the line Yp and the axis of fatigue steel wire. As shown in Fig 5, the volume between the paraboloid P and the cylinder Q is the wear volume of the fatigue steel wire. The geometric model was established by employing Pro/E software, then the wear volume V can be got by the software.

The equation of the cylinder Q in the three-dimensional system of coordinate X_QY_QZ is

$$x^2 + z^2 = 250000 \tag{1}$$

The equation of the paraboloid P in the three-dimensional system of coordinate X_PY_PZ is

$$z = \frac{4h}{L^2} - h + 500 \tag{2}$$

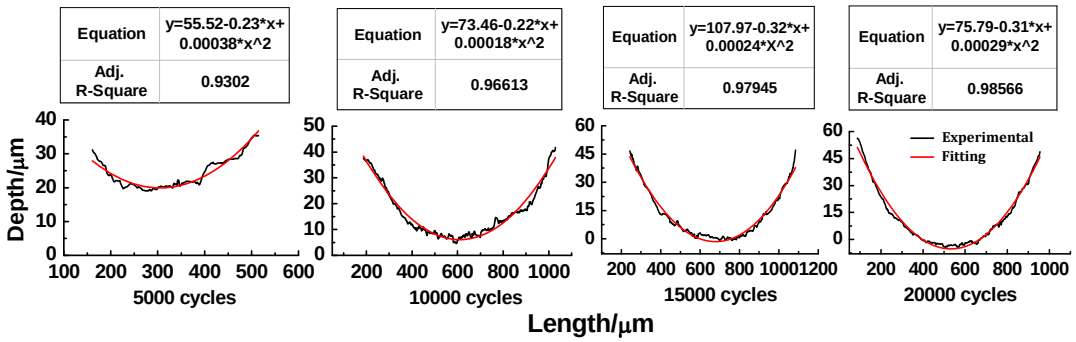

Fig 4. Polynomial fitting of wear depth profiles of fatigue wires in tests at different fatigue cycles

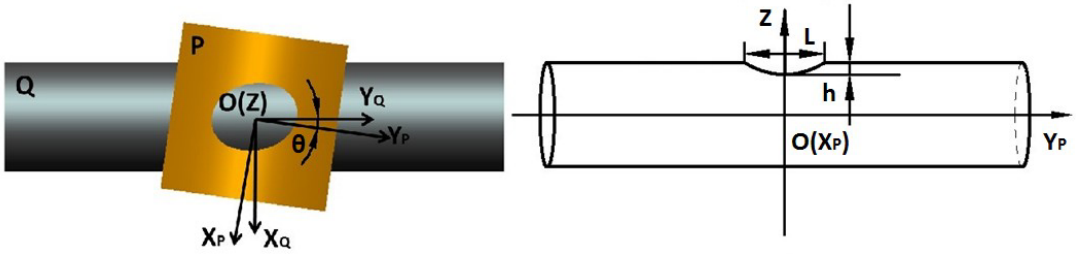

(a)Three dimensional geometric model (b) Wear depth of geometric model

Fig 5. Geometric model of the wear scar

In order to quantitatively analyze the degree of wear of fatigue steel wire, the wear coefficient kcof, i.e. wear volume per unit relative slip per unit contact load, is introduced[9]

$$k_{cof} = \frac{V}{S_x F_n} = \frac{V}{2\Delta x N F_n} \tag{3}$$

Where Sx is the total stroke of relative slip, Fn is the contact load, Δx is the relative slip range between contacting wires.

The wear coefficients of fatigue steel wires during multi-axial fretting-fatigue were obtained by using Eq. (3) (Fig 6). It is shown in Fig 6 that the wear coefficient increases quickly at first and then tends to be stable when the fatigue cycles increases from 5000 to 20000. At the start of fretting, the oxidation film and the stain on surface of the fatigue steel wire have an anti-friction effect[10], the contact between steel wires are comparatively large micro convex peak contact, which will reduce the real contact area and the removing speed of material, so the wear coefficient is low at the start of fretting. As the fatigue cycle increases, the surface protective film will rupture and the micro convex peak will be removed, which will increases the real contact area and the removing speed of material, so the wear coefficient will increases. As the fatigue cycle increases to a certain degree, wear debris bed and oxidation of the surface of the wear scar play a adjust role in the wear, which will result in the stable of the wear coefficient [11, 12].

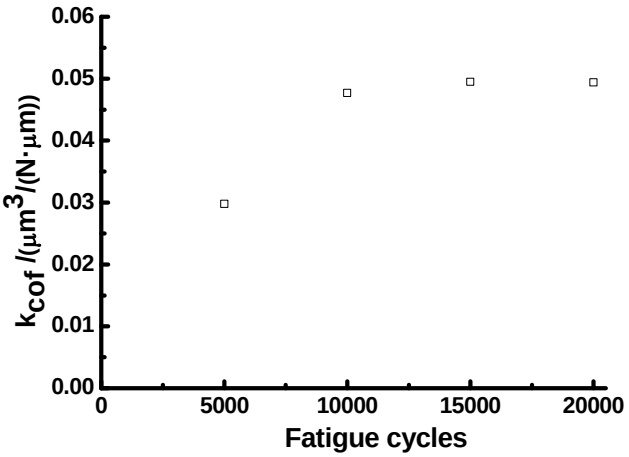

Fig 6. Wear coefficients of fatigue wires at different fatigue cycles

Acknowledgements
The research reported here was supported by the National Natural Science Foundation of China (51405489; 51375479) and Tribology Science Fund of State Key Laboratory of Tribology (SKLTKF13A04).

References
[1] Wang D. G., Li X. W., Wang X. R., Shi G. Y., Mao X. B., and Wang D. A. 2016. "Effects of hoisting parameters on dynamic contact characteristics between the rope and friction lining in a deep coal mine," Tribol Int, 96:31–42.
[2] Wang D. G., Zhang D. K., and Ge S. R. 2011. "Fretting-fatigue behavior of steel wires in low cycle fatigue," Mater Des, 32:4896–993.
[3] Li T., Miao Y. J., and He G. D. 2010. "Preliminary exploration to reason for early breaking of wires in deep shaft," Coal Mine Machinery, 31(11): 94-96.
[4] Wang D. G. 2015. "Study on mechanical modelling and fretting fatigue damage behaviors of hoisting rope," Central South University Press, Changsha.
[5] Zhang, J., Wang, D. G., Zhang, D. K., Ge, S. R. and Wang D. A. 2017. "Dynamic torsional characteristics of mine hoisting rope and its internal spiral components," Tribol Int, 109: 182-191.
[6] Liu B., He G. Q., and Jiang X. S. 2012. "Multi-axial fretting fatigue behavior". J Tongji Univ: Nat Sci, 40(1): 77-80.
[7] Wang D.G., Zhang D.K., and Ge S.R. 2014. "Effect of terminal mass on fretting and fatigue parameters of a hoisting rope during a lifting cycle in coal mine," Eng Fail Anal, 36: 407–422.
[8] Shen M. X., Xie X. Y., Cai Z. B., Mo J. L., and Zhu M. H.2011. "Experimental study and simulation of dual-rotary fretting," J Mech Eng, 47(15): 89-94.
[9] Wang D. G., Zhang D. K., Wang S. Q., and Ge S. R.2013. "Finite element analysis of hoisting rope and fretting wear evolution and fatigue life estimation of steel wires ," Eng Fail Anal, 27(1): 173–193.
[10] Wang L. 2014. "Research on wear behavior and wear mechanism of titanium alloys," Jiangsu University, Zhenjiang.
[11] Gnanamoorthy R., and Reddy R. R. 2002. "Fretting fatigue in AISI 1015 steel," B Mater Sci, 25(2): 109-114.
[12] Jin O., andMall S. 2002. "Effects of independent pad displacement on fretting fatigue behavior of Ti–6Al–4V," Wear, 253(5): 585-596.